ACS OMEGA

Article

Cite This: ACS Omega 2019, 4, 16441−16449

http://pubs.acs.org/journal/acsodf

Polyethylenimine-Modified Zeolite 13X for CO_2 Capture: Adsorption and Kinetic Studies

Swetha Karka,[†] Sudarshan Kodukula,[†] Satyanarayana V. Nandury,[†] and Ujjwal Pal*[,†,‡]

[†]Department of Energy and Environmental Engineering, CSIR-Indian Institute of Chemical Technology, Hyderabad 500007, India

[‡]Academy of Scientific and Innovative Research (AcSIR), New Delhi 110001, India

Supporting Information

ABSTRACT: A class of high molecular weight polyethylenimine (PEI)-modified zeolite 13X adsorbents were synthesized by varying the concentration of imines and screened for preliminary investigation of CO_2 capture studies. The impregnated molecular amine zeolite composite was characterized and CO_2 adsorption performance was investigated through TGA in the presence of atmospheric pure CO_2 gas at 25, 50, 75, and 100 °C, respectively, using 20−80 wt % of PEI-loaded zeolite 13X adsorbents. This paper reports on the effects of temperature and amine (PEI) loading on CO_2 adsorption capacity and estimated kinetic parameters through modeling of selected models which represent the reaction rate and diffusion rate models. The studied adsorbents showed the highest adsorption capacity at 75 °C with 60 wt % PEI loading. Thus, the optimum temperature of 75 °C and optimal loading of 60 wt % was observed from the current studies for CO_2 capture. From modeling study, it was found that Avrami's fractional order and dual kinetic models (DKM) described well the adsorption behavior of CO_2 on PEI-impregnated zeolite 13X at all temperatures accurately and up to 75 °C, respectively. Besides, intraparticle diffusion was found to be the rate-limiting step when compared with the film diffusion model.

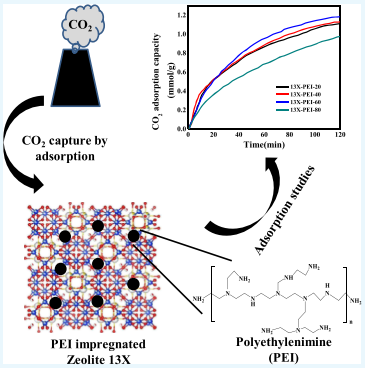

1. INTRODUCTION

Coal facilitates security and access for energy in most developed and developing economies throughout the world but symbolizes the major source of carbon emissions which is threatening to the climate system. In spite of the implementation of recent environmental policies of some developed countries for reduction in coal use, the world is still mostly depending on to coal, which is primarily used for electricity generation and, to some extent, for the production of cement, chemicals, steel, and liquid fuels.[1,2] To use coal in a sustainable manner in the coming future, there is a need for developing a technology which reduces the associated CO_2 emissions from coal power plants, and this can be achieved through the execution of carbon capture, utilization, and storage technologies.[3−6]

Postcombustion capture-based technology is considered widely for carbon dioxide capture from flue gases. In this technology, CO_2 from flue gas is captured after the fossil fuel has been burned. There are four pathways to capture CO_2 under post-combustion technology, which are absorption, adsorption, cryogenic distillation, and membrane purification.[7] Among the varied pathways, the most matured technology to separate CO_2 from flue gas is absorption based, wherein liquid amines are circulated in adsorption and stripping column in a cycle. Nevertheless, this pathway using liquid amine has been used for CO_2 capture industrially for decades, has a number of defects such as intense corrosive nature of amines on equipment and high-energy requirement for the regeneration of amine solution.[8] Therefore, to get over from their limitations, adsorption is chosen as one of the most likely routes because of the relatively less energy requirement, lower cost involved in adsorbent preparation, and wider applicability in terms of operating temperature and pressures. There are plenty of materials that have been studied for CO_2 adsorption such as zeolite,[9] metal−organic frameworks,[10] activated carbon,[11,12] alkaline metal oxides,[13,14] and amine−silica hybrid/composite adsorbents.[15] Amid these adsorbents, zeolite has been investigated mostly and especially zeolite 13X, which has been regarded as a benchmark material for CO_2 capture because of its high CO_2 adsorption capacity. In spite of this feature, zeolite is found to be more effective at ambient temperature as physical adsorption is more predominant in these materials and less effective at higher temperatures. In view of this drawback and to make zeolite operational at higher temperatures and near atmospheric pressures (real flue gas conditions), suitable amine-modified/-impregnated zeolite is prepared and tested for their capacity in this present study, as these prepared materials would act as a hybrid adsorbent, wherein both physisorption and chemisorption would take place.[16]

The studies on amine-modified adsorbents have earned significant attention in CO_2 capture research area because of its simple chemistry involved between the acidic CO_2 molecule and basic amine molecule impregnated on the solid surface.

Received: July 4, 2019
Accepted: September 13, 2019
Published: September 25, 2019

DOI: 10.1021/acsomega.9b02047
ACS Omega 2019, 4, 16441−16449

Majority of the research has been focused on improving the CO_2 adsorption capacity and selection of relevant amine for surface modification. There has been substantial research progressing in the area of basic amine groups and zeolite.[17−20] Recently, diverse amines have been used in the synthesis of amine−zeolite adsorbents, including monoethanolamine (MEA), tetraethylenepentamine, polyethylenimines (PEIs), an so forth. Jadhav et al.[16] studied adsorption capacities of impregnated MEA onto zeolite 13X-based adsorbents in the temperature range of 30−120 °C. The sorbents exhibited betterment in CO_2 adsorption capacity over the pristine zeolite by a factor of 1.6 at 30 °C and at 120 °C by a factor of 3.5 in CO_2 capture efficiency. Chen et al.[21] modified 13X zeolite by using a mesopore-generating agent and then with PEI_{800MW}. It is found that the mesoporous 13X zeolite showed better CO_2 capture capacity and selectivity at high temperature (e.g., 100 °C) with dilute CO_2 concentrations.

In recent research, PEI has drawn great attention in CO_2 capture study using different supports because of its easily synthesizable property, relatively less cost and lastly because of its high thermal stability when compared with other amines.[22] Li et al. has considered the influence of the PEI type (linear or branched) and molecular weight on the CO_2 capture performance. It was observed that the CO_2 adsorption capacity diminished with the increasing PEI molecular weight, and branched PEIs had higher sorption capacities than linear PEIs because of their greater mobility. It was also found that branched PEI of 800 molecular weight with the silica support showed highest CO_2 sorption capacity of 202 mg of CO_2/g of the adsorbent at 105 °C under pure CO_2 atmosphere.[23]

In the present work, ($PEI_{600000MW}$) of higher molecular weight is impregnated on 13X zeolite to study its adsorption capacity and kinetics. It is expected that this novel adsorbent would adsorb better than pristine zeolite, especially at higher temperatures. This study could be considered as preliminary experimentation on higher molecular weight amine-impregnated zeolite for CO_2 adsorption at atmospheric pressures along with the kinetic modeling studies for this particular class of sorbents. Amine impregnation on zeolite is verified through prominent characterization techniques.

2. EXPERIMENTAL SECTION

2.1. Materials. The amine used in the synthesis of the adsorbent was of analytical grade PEI solution (~50% in H_2O) of molecular weight ranging between 600 000 and 1 000 000, which was procured from Sigma-Aldrich, India, and was used as such without any further purification. The solvent used was methanol procured from Finar Limited, India, was distilled to obtain anhydrous methanol for adsorbent preparation. Zeolite 13X powder of nearly 2 μm average particle size was procured from Sigma-Aldrich, India. Carbon dioxide and nitrogen gas cylinders were purchased from Vijay Enterprises, Secunderabad, Telangana, India.

2.2. Synthesis of Amine-Immobilized Adsorbents. PEI was anchored on commercial zeolite 13X through a physical impregnation method as mentioned by Xu et al.[24] and the schematic representation of the preparation method is shown in Figure 1. The immobilization of amine (PEI) on zeolite was carried out using an alcoholic solution of amine. A given amount of amine was dissolved in distilled methanol and stirred for 30 min. The zeolite of 1 g quantity was added to this alcoholic solution and the resulting slurry was stirred continuously for 24 h. A solid−liquid ratio of 1:2 was

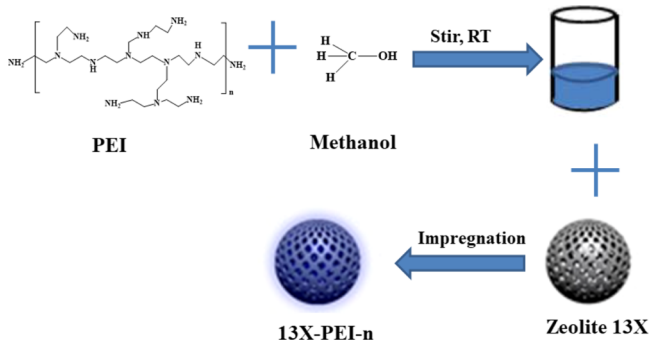

Figure 1. Schematic representation of adsorbent preparation.

maintained during the adsorbent's preparation. The amine solution was then filtered and the modified zeolite slurry was dried in an oven at 70 °C for 3−4 h. The prepared adsorbents were named as 13X-PEI-*n*, where *n* represents the loading of PEI as the weight percentage in the sample.

2.3. Sorbent Characterization. Different characterization techniques were considered to obtain a useful comparison between amine-modified and -unmodified zeolite 13X. Those techniques were N_2 adsorption/desorption isotherms, X-ray powder diffraction (XRD), Fourier-transform infrared spectroscopy (FTIR), scanning electron microscope (SEM), transmission electron microscopy (TEM), thermo-gravimetric analysis (TGA), and elemental (CHNS) analysis.

Nitrogen adsorption/desorption isotherms were measured using an Autosorb apparatus for the determination of textural properties such as surface area (S_{BET}), total pore volume (V_{TOTAL}), and mean pore volume (V_{MEAN}). The impregnated adsorbents were initially outgassed at 423 K, to avoid amine volatilization, and then subjected to stepwise N_2 gas at 77 K. Thermogravimetric analysis was performed using the TA Instruments SDT Q600 apparatus to study the thermal stability of the synthesized adsorbents and even to determine the amine loading. Around 15−20 mg of the sample was placed in theTG pan and was heated at a rate 10 °C/min in an inert atmosphere of nitrogen gas. The samples were heated starting from 25 to 1000 °C. The adsorbent's weight loss was recorded. The FTIR spectra of the prepared materials were recorded using a Thermo Nicolet Nexus 670 spectrometer using the KBr pellet technique. The wavelength region of 4000−400 cm^{-1} was considered for analysis. A diffractometer with monochromatic Cu Kα radiation (k = 1.54 Å) was considered for powder X-ray diffraction studies. The total carbon, nitrogen, hydrogen and sulphur content were determined using a CHNS analyzer of the Elementar Vario MICRO cube model. SEM analysis is carried out using a Hitachi S-3000N SEM to study the morphology of the samples. TEM analysis is carried on FEI of Talos make.

2.4. Kinetics. *2.4.1. Adsorption Kinetics.* Through kinetic analysis, gas adsorption rate defines the residence time required for completeness of the adsorption reaction. The mathematical models which define the adsorption data can be classified as adsorption reaction models and adsorption diffusion models.[27] Though both categories of models describe the kinetic process of adsorption, they represent the different nature of the kinetic analysis. In case of reaction models, experimental data would be fitted with differential equations like pseudo-first order, pseudo-second order, and so forth, which helps in knowing the reaction order and rate constants. At present, more evolved reaction models are developed to

DOI: 10.1021/acsomega.9b02047
ACS Omega 2019, 4, 16441−16449

describe the kinetic process of adsorption, whereas adsorption diffusion models are based on three consecutive steps: (a) external diffusion or film diffusion, that is, diffusion across the gas film surrounding the adsorbent particle, (b) internal diffusion or intraparticle diffusion, that is, diffusion of gas in the pores and/or along the pore walls and (c) mass action, that is, adsorption and desorption between the gas molecules and active sites.

In the current study of kinetics, we have considered linear driving force model (LDF), Avrami's fractional order, and dual kinetic model (DKM) under reaction models category whereas Boyd and intraparticle diffusion models under diffusion models.

2.4.1.1. Linear Driving Force Model. The LDF is the most common and widely used equation for gas-solids systems and was assumed to follow first-order kinetics.[28] The model is represented by eq 1.

$$\frac{\partial q_t}{\partial t} = k_1(q_e - q_t) \tag{1}$$

where q_e and q_t are the adsorption capacity at equilibrium and at time t, respectively, and k_1 is mass transfer constant. For the boundary conditions $q_t = 0$ at $t = 0$ and $q_t = q_e$ at $t = \infty$ the integrated form of eq 2 becomes

$$q_t = q_e(1 - e^{-k_1 t}) \tag{2}$$

2.4.1.2. Avrami's Fractional Order Kinetic Model. This model is developed to simulate phase transition and crystal growth of materials. However, it can also be considered to describe the adsorption of CO_2 on amine-functionalized adsorbents. The differential form of this model is as follows[29]

$$\frac{\partial q_t}{\partial t} = k_A{}^{n_A} t^{n_A - 1}(q_e - q_t) \tag{3}$$

where n_A is the Avrami exponent and k_A is the Avrami kinetic constant. The Avrami exponent, n_A, is a fractional number, which speculates mechanism changes that may take place during the adsorption process. Here, n_A is the dimensionality of growth of adsorption sites: $n_A = 2$ for one-dimensional growth, $n_A = 3$ for two dimensional growth, and $n_A = 4$ for three-dimensional growth. For homogeneous adsorption in which the probability of the adsorption to occur is equal for any region for a given time interval, $n_A = 1$. The integrated form of the above equation is

$$q_t = q_e(1 - e^{-(k_A t)^{n_A}}) \tag{4}$$

2.4.1.3. Dual Kinetic Model. It is a new semi-empirical model which is particularly considered for amine-functionalized solid materials, wherein several overlying processes which influence the adsorption kinetics are taken into consideration.[30] According to this model, the overall adsorption q_t is the combination of surface q_{sur} and bulk sorption q_{bulk}

$$q_t = q_{sur} + q_{bulk} \tag{5}$$

Then, the time derivative is given as follows

$$\frac{\partial q_t}{\partial t} = \frac{\partial q_{sur}}{\partial t} + \frac{\partial q_{bulk}}{\partial t} \tag{6}$$

Here, q_{sur} is defined as the CO_2 uptake at the surface and q_{bulk} as the CO_2 adsorption in the bulk phase of the sorbent. Both terms correspond to physisorption and chemisorption at varied sites within the amine layer. As adsorption can be described as a reaction of higher order, kinetics of surface sorption can be depicted using a fractional-order kinetic approach

$$\frac{\partial q_{sur}}{\partial t} = k_{sur}(q_e - q_t)^{n_{DKM}} \tag{7}$$

Besides surface sorption, the physical and chemisorbed CO_2 molecules can further react with active sites present on the bulk amine layer and these interactions can be accounted as follows

$$\frac{\partial q_{bulk}}{\partial t} = k_{bulk} q_t (q_e - q_t)^{n_{DKM}} \tag{8}$$

Combining equations eqs 7 and 8 we get

$$\frac{\partial q_t}{\partial t} = k_{sur}(q_e - q_t)^{n_{DKM}} + k_{bulk} \cdot q_t \cdot (q_e - q_t)^{n_{DKM}} \tag{9}$$

On rearranging the above equation, we drive our dual kinetic model

$$\frac{\partial q_t}{\partial t} = k_{DKM} \cdot (1 + \beta_{DKM} \cdot q_t) \cdot (q_e - q_t)^{n_{DKM}} \tag{10}$$

where, k_{DKM} is the constant for the dual kinetic model β_{DKM} is the ratio of k_{bulk} and k_{sur}. This model is solved using Euler's numerical method as the derived DKM model equation is a first-order first-degree differential equation with an initial value of $q_t = 0$ at $t = 0$.

2.4.1.4. Boyd Model. Boyd developed a model to understand whether film diffusion or intraparticle diffusion is the rate-controlling step in adsorption kinetics.[31] This model is based on the assumption that the boundary layer on the adsorbent surface has a significant effect on the diffusion of a gas. This effect is determined as follows

$$F = 1 - \frac{6}{\pi^2}\sum_{1}^{\infty}\frac{1}{n^2}\exp(-n^2 B_t) \tag{11}$$

Here, F is the fraction of CO_2 gas adsorbed at time t (q_t) to CO_2 gas adsorbed at an infinite time, that is, at equilibrium (q_e). B_t is a mathematical function of F and it is calculated using the integrated Fourier transform of eqs 13 and 14.

$$F = \frac{q_t}{q_\infty} \tag{12}$$

$$0 \le F \le 0.85: \qquad B_t = 2\pi - \frac{\pi^2 F}{3} - 2\pi\left(1 - \frac{\pi F}{3}\right)^{1/2} \tag{13}$$

$$0.86 \le F \le 1: \qquad B_t = -0.4977 - \ln(1 - F) \tag{14}$$

The rate-limiting step is predicted by the plotting B_t versus t. If the plot shows linearity with the graph passing through the origin, then the rate-limiting step is considered to be intraparticle diffusion, otherwise the film diffusion model governs the process. The slope of the B_t versus t graphs passing through origin represents the time constant value, that is, B, using which the effective diffusion coefficient (D_i) can be calculated at different temperatures using the following equation.

DOI: 10.1021/acsomega.9b02047
ACS Omega 2019, 4, 16441−16449

$$B = \frac{\pi^2 D_i}{r^2} \tag{15}$$

Here, r is the radius of the adsorbent particle.

2.4.1.5. Intraparticle Diffusion Model. Weber−Morris found this model and is applicable in many adsorption cases. According to this model, gas uptake (q_t) varies proportionally with half power raised to time ($t^{1/2}$).

$$q_t = k_{\text{int}} t^{1/2} \tag{16}$$

Here, k_{int} is the intraparticle diffusion rate constant.

As per this model, the graph of q_t versus $t^{1/2}$ should be linear passing through the origin for considering intraparticle diffusion as the rate-controlling step. If the graph does not pass through the origin, then it is an indication that different mechanisms may control the rate of adsorption which may be operating simultaneously along with intraparticle diffusion. From this model, the diffusion coefficient for intraparticle diffusion of gas adsorption within the pores of amine-modified zeolite can be calculated by employing the following equation.[32]

$$D_p = \frac{0.03 \times r^2}{t_{1/2}} \tag{17}$$

where D_p is the diffusion coefficient (cm^2/s), $t_{1/2}$ is the time (s) for half-adsorption of CO_2 on adsorbent, and r is the average radius of the adsorbent particle in cm. The value of r is taken as 2×10^{-4} cm for the current study.

2.4.2. Desorption Kinetics. Desorption is equally important along with adsorption for the design of temperature or pressure swing adsorption processes as it is contributing to the total energy consumption, that is, heating and/or vacuum and its kinetic analysis demonstrates the time required for complete regeneration of a process. Desorption kinetic modeling studies are addressed by very few researchers to date. Few of the models which were investigated and considered for the present class of the adsorbent are as follows.

2.4.2.1. First-Order Model. Generally, CO_2 desorption obeys first-order kinetics and its expression is represented as follows.[33]

$$q_{\text{des}} = q_o \, e^{-k_{\text{des}} t} \tag{18}$$

Here, q_{des} is the mass of CO_2 desorbed at time t and q_o is the mass of CO_2 at maximum adsorption, and k_{des} is the desorption rate constant.

2.4.2.2. Avrami's Model. This model is studied particularly for amine-functionalized materials and it can be described by the following equation[30]

$$\Theta = 1 - \exp(-(k_A t)^{n_A}) \tag{19}$$

Here, Θ represents the ratio of the current loading during desorption $q_{t,\text{Des}}$ and the loading at the end of the adsorption step $q_{t,\text{Ads}}$.

3. RESULTS AND DISCUSSION

3.1. Sorbent Characterisation. SEM and TEM images of pristine zeolite 13X and modified zeolite 13X image varied compositions of amine is presented in Figure S1. From SEM analysis, the images reflect a crystal-like surface morphology. It was observed that there is no significant change before and after impregnation which indicates that PEI impregnation did not change much of the morphology of the zeolite. The zeolite 13X image resembled well with that of the reported image found in the literature,[34] whereas, from TEM images, it is observed that a PEI based molecular layer was laid on solid surface of modified zeolite and along with observed depleted crystallinity in the modified phase (Figure S1c,d). Infrared spectra (Figure S2) showed that the samples have both amines and zeolite features, indicating that PEI was impregnated considerably in zeolite 13X. XRD spectra (Figure S3) show several Bragg peaks at angles between 2° to 40° 2θ degree which is typical for any zeolite material. After the PEI was loaded, the intensity of the diffraction peaks of the zeolite 13X reduced substantially, which was presumably induced by the PEI's dense layer formation on the surface of zeolite 13X.

3.1.1. N_2 Adsorption/Desorption Isotherms. Figure 2 shows the N_2 adsorption−desorption isotherms of the zeolite

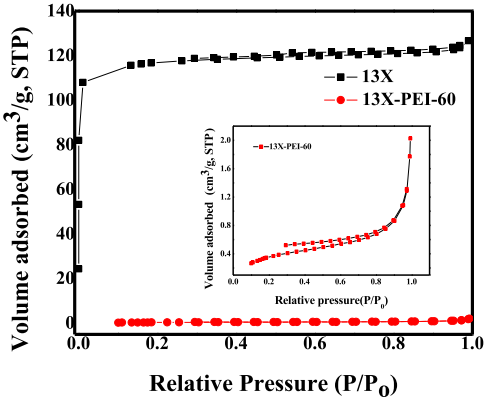

Figure 2. N_2 adsorption−desorption isotherms at 77 K, (inset) of 13X-PEI-60.

13X and 60 wt % PEI-modified zeolite 13X (13X-PEI-60). Zeolite 13X showed typical Type I isotherm as per the IUPAC classification with most microporous features as found out by the high volume of N_2 adsorption at very low relative pressures. As the synthesis is carried out by physical impregnation, it is more likely that a thick layer of PEI molecules would have been engulfed over the zeolite 13X surface which could prevent N_2 sorption at low temperatures of 77 K. The corresponding textural properties of the samples are tabulated in Table 1.

Table 1. Textural Properties of Sorbents

sample	S_{BET} (m^2/g)	V_{TOTAL} (cm^3/g)	V_{MEAN} (nm)
13X	437	0.20	1.8
13X-PEI-60	1.31	0.003	11.6

3.1.2. Thermo-Gravimetric Analysis. Figure S4 depicts the thermal behavior of pristine zeolite 13X and amine impregnated zeolite 13X measured by TGA under dry N_2 environment. The samples were heated from 25 to 800 °C by a speed of 10 °C per min. As can be seen, the Figure S4 zeolite 13X showed a two-step decomposition process (weight loss of 25.16%) in the temperature range 25−400 °C and that can be attributed to the desorption of both physi- and chemisorbed water molecules. On the other hand, zeolite 13X with 20, 40, 60, and 80% amine impregnation showed multistep decomposition with a weight loss % of 26.64, 26.57, 26.35, and 32.27, respectively, in the same temperature range. Because zeolite

DOI: 10.1021/acsomega.9b02047
ACS Omega 2019, 4, 16441−16449

13X-PEI-60 showed maximum adsorption of CO_2, detailed analysis by TGA coupled to mass spectroscopy (MS) was carried out to understand the decomposition pattern of PEI from the evolved gas fragments at various stages and the observed TGA−MS thermogram is shown in the Figure 3.

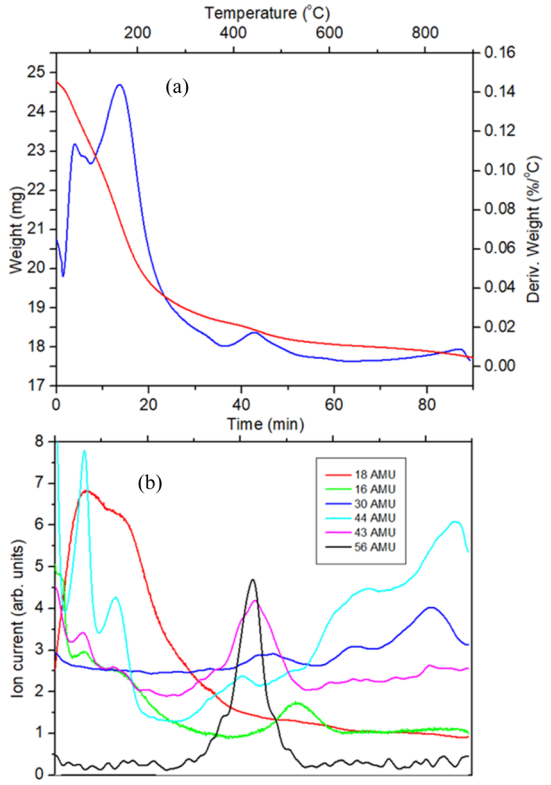

Figure 3. (a) TGA−DTG analysis for 13X-PEI-60 and (b) MS analysis for 13X-PEI-60.

As can be seen from the TGA−MS thermogram (Figure 3) of zeolite 13X-PEI-60 that it undergoes three step decomposition process at 25−100, 100−400 and 400−600 °C. Along with H_2O (18 AMU), mass fragments $-NH_2$ (16 AMU), $-CH_2-NH-CH_2-$ (43 AMU) and $-CH_2-CH_2-NH_2$ (44 AMU) are also observed between 25 and 400 °C, which clearly indicated the decomposition of PEI. During the third decomposition step, that is, 400−600 °C, in addition to the above mass fragments, $-N-(CH_2)_3-$ (56 AMU) is also observed, inferring that the PEI molecule is adsorbed on to the zeolite 13X both physically and chemically as decomposition of the PEI molecule is taking place at low and high temperatures.

Table S1 presents the amine loading of amine-impregnated zeolite 13X samples of different weight percentage of amine used, determined through TGA. Amine loading of each impregnated sorbent was calculated using TGA as the weight drop from 100 to 800 °C and then changing it into a dry mass base at 100 °C.[21]

3.1.3. Elemental Analysis. The results of elemental analysis are tabulated in Table 2. It is observed that the amine loading has been successful in the zeolite structure through the presence of nitrogen content (1.43 to 2.18 wt %) and carbon content (2.73 to 3.98 wt %) in the PEI-impregnated zeolite 13X.

3.2. CO_2 Adsorption by PEI-Impregnated Zeolite 13X.

3.2.1. Effect of Adsorption Temperature on CO_2 Adsorption Capacity. Figure 4 shows CO_2 adsorption capacities of 20, 40, 60, and 80 wt % PEI-impregnated zeolite 13X using 99.99% pure CO_2 gas at different temperatures of 25, 50, 75, and 100 °C. The maximum CO_2 adsorption from the experiment was observed around 75 °C, which indicates that 75 °C could be considered as the optimum adsorption temperature for CO_2 adsorption for the current class of sorbents. It was found that CO_2 adsorption for all the amine-loaded sorbents increased with increasing temperatures till 75 °C and later decreased by reaching 100 °C. The nature of highly loaded sorbents at temperatures up to 75 °C is related with the diffusion-controlled mechanism as the pores get occupied with PEI, which limits the availability of amine sites for CO_2 adsorption. The high CO_2 adsorption capacities for these highly loaded sorbents (40 and 60 wt %) can be attributed to reduced diffusion resistance with the increase in temperatures,[15] whereas at the higher temperature (100 °C), the low CO_2 adsorption capacity can be attributed to the exothermic nature of the reaction. It was seen that at a lower temperature of 25 °C, lower loaded amine of 20 wt % PEI, and at higher temperature of 100 °C, higher loaded amine of 80 wt % showed higher adsorption capacities of 1 and 0.36 mmol/g, respectively. Thus, it can be generalized that at low temperature, sorbents with low PEI loading might be more advantageous, and at high temperature, sorbents with high PEI loading might be more advantages for CO_2 capture. Table S1 shows the CO_2 adsorption capacity of varied amine-loaded zeolite 13X at 75 °C and 1 atm and Table S2 shows CO_2 adsorption capacity for all different loadings of PEI on zeolite 13X at different temperatures.

Table 2. Elemental Analysis for Zeolite 13X and PEI-Impregnated Zeolite

sample ID	nitrogen (wt %)	carbon (wt %)	hydrogen (wt %)
13X	0.00	0.00	2.65
13X-PEI-20	1.43	2.73	2.95
13X-PEI-40	1.50	2.72	2.89
13X-PEI-60	2.03	3.76	3.10
13X-PEI-80	2.18	3.98	3.11

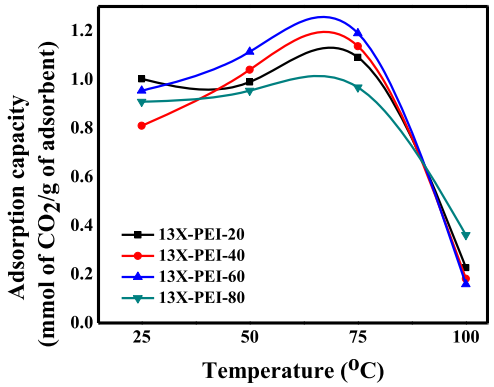

Figure 4. CO_2 adsorption capacity of different loadings of PEI on zeolite 13X at different temperatures.

3.2.2. Effect of PEI Loading on CO_2 Adsorption Capacity. Zeolite 13X support with varied PEI loading was prepared to find out the effect of amine loading on CO_2 adsorption capacity. It is observed that CO_2 adsorption capacities increases as the amine loadings increased from 20 to 60 wt

DOI: 10.1021/acsomega.9b02047
ACS Omega 2019, 4, 16441−16449

Table 3. Comparison of Adsorption Capacities for PEI-Loaded Adsorbents

adsorbent	amine loading (wt %)	CO_2 adsorption capacity (mmol/g)	temperature (°C)	pressure (atm)	references
13X		0.36	75	1	19
13X-MEA	50	0.45	75	1	19
Meso-13X-PEI_{800MW}	33	1.32	75	1	21
13X-$PEI_{600000MW}$[a]	60	1.22	75	1	this study
SBA-$PEI_{750000MW}$	20	2.15	75	1	35
MCM41-PEI	50	2.55	75	1	22

[a]The adsorption capacity was measured by TGA under a pure CO_2 atmosphere at a flow rate of 50 mL/min.

% and sorbent with 60 wt % PEI obtained the highest CO_2 uptake. However, for PEI loading beyond 60 wt %, there was a reduction in the adsorption capacity because of maximum pore blocking in the zeolite structure. The amine loading of 60 wt % showcased maximum CO_2 adsorption capacity of 1.22 mmol/g of the adsorbent in pure CO_2 gas at 75 °C and 1 atm pressure (Table 3).

3.2.3. Adsorption Kinetics. The kinetics of CO_2 adsorption of the prepared sorbents should be fast enough to capture CO_2 in practical applications. Figure 5 represents CO_2 adsorption

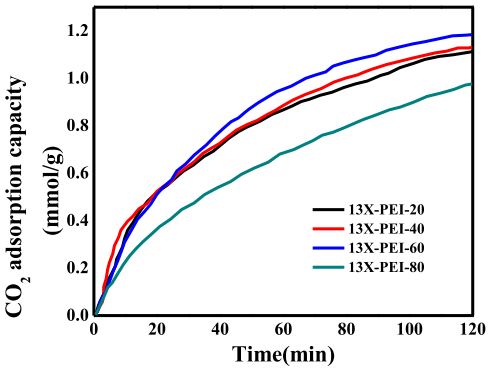

Figure 5. CO_2 adsorption capacity as a function of time of different PEI loading on zeolite 13X at 75 °C and 1 atm.

capacity of zeolite 13X with varied PEI loadings as a function of time in the presence of 99.99% pure CO_2 gas at 75 °C and 1 atm pressure. As can be observed from Figure 10, CO_2 adsorption capacity for all PEI-loaded sorbents increases gradually with respect to time, with 60 and 80 wt % PEI-loaded sorbents, showing fastest and slowest adsorption rates respectively. The adsorbent with 60 wt % PEI loading adsorbed 0.93 mmol/g at the end 60 min, whereas 80 wt % PEI loading adsorbed 0.67 mmol/g at the same time. The better kinetics of 60 wt % PEI-loaded sorbent can be attributed to diminished diffusion resistance during CO_2 adsorption on the sorbent as discussed earlier, whereas, for 80 wt %, the PEI-loaded sorbent took longer time to reach adsorption capacity of nearly 1 mmol/g which might be due to heavy blocking of the microchannels by PEI molecules for the CO_2 molecules to approach or diffuse to the surface and react with the available amine groups.

3.3. Kinetic Modeling. Theoretically, the adsorption of CO_2 on PEI-impregnated zeolite 13X can be described with any of the three reaction models mentioned earlier. Figure 6 shows the CO_2 uptake of PEI-impregnated zeolite 13X at 75 °C and with 60 wt % amine loading along with the curves generated by fitting the three models. Kinetic parameters, as well as squared correlation coefficient (R^2) for regressions, were listed in Table 4. From the results, it can be concluded

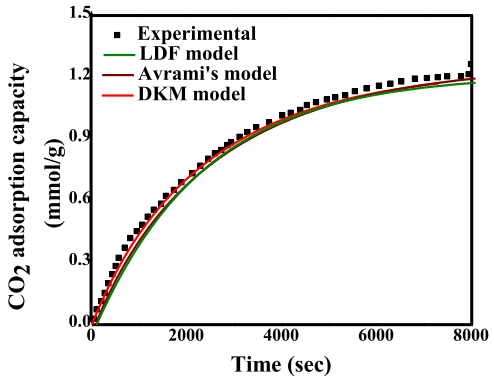

Figure 6. Adsorption behavior predicted by different reaction kinetic models at 75 °C of 13X-PEI-60.

that the Avrami's fractional order kinetic model shows the best fit which describes the adsorption behavior of CO_2 on PEI-impregnated zeolite 13X at all temperatures. However, the DKM model also offers the best description of the given system except at 100 °C, where the model unfit can be attributed to a low rate of CO_2 adsorption.

The mass transfer constant k_1 of the LDF model increased with increasing temperature which indicates better adsorption at higher temperatures of about 50 to 75 °C. The Avrami's exponent n_A from curve fitting ranged between 0.62 to 1.74 which on an average valued to 1.01. This indicates homogeneous adsorption of solute which would occur for any region for a given time interval, whereas in the case of the DKM model, kinetic constant k_{DKM} increases and interaction parameter β_{DKM} decreases with the temperature, respectively.

The temperature dependence of the kinetic constant k_A is described by the Arrhenius equation.[36]

$$k_A = A\, e^{-(E_a/RT)} \tag{20}$$

where A is the Arrhenius pre-exponential factor, E_a is the activation energy, R is the universal ideal gas constant, and T is the absolute temperature. The plot of $\ln(k)$ versus $1/T$ is shown in Figure 7 and the value of E_a is given in Table 6.

From the Boyd model study, it was observed from Figure 8 that B_t versus t graph passed through the origin, which indicates that the rate-controlling step is intraparticle diffusion. However, it is found in many studies that film diffusion plays a role as a limiting step during the initial stages of adsorption and then followed by intraparticle diffusion when gas molecules reach the surface of the adsorbent. In addition to this observation, this model helps in determining the effective diffusion coefficient (D_i) according to eq 15 and whose values are tabulated in Table 5. The D_i values would be used to find the activation energy E_a (given in Table 6) by plotting ln D_i versus $1/T$ as per the following equation.[37]

DOI: 10.1021/acsomega.9b02047
ACS Omega 2019, 4, 16441−16449

Table 4. Kinetic Parameters of Reaction Models by the 13X-PEI-60 Sorbent

model	parameter	25 °C	50 °C	75 °C	100 °C
LDF model	k_1 [10^{-4} s^{-1}]	4.04	4.12	4.28	7952
	q_e [mmol/g]	1.331	1.31	1.229	0.1181
	R^2	0.9643	0.9811	0.9983	0.0001
Avrami's order	k_A [10^{-4} s^{-n_A}]	1.07	2.71	3.93	22.6
	n_A [-]	0.6246	0.7897	0.9221	1.743
	q_e [mmol/g]	2.3	2.1	1.278	0.1573
	R^2	0.9958	0.9922	0.9991	0.9895
DKM model	k_{DKM} [10^{-4}·s^{-1}·$mmol^{1-n}$ DKM·g^{nDKM-1}]	2.82	5.10	5.21	6.01
	β_{DKM} [g·$mmol^{-1}$]	−0.54	−0.581	−0.587	−0.5
	n_{DKM} [-]	0.4226	0.5503	0.62	0.9
	R^2	0.9812	0.9875	0.9988	0.7242

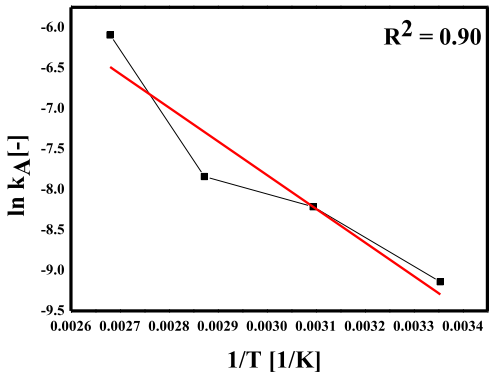

Figure 7. Arrhenius plots for the kinetic constants obtained by Avrami's fractional kinetic model for 13X-PEI-60.

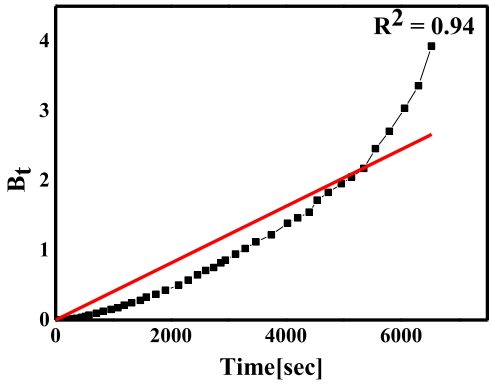

Figure 8. Curve fitting of the Boyds model for 13X-PEI-60 at 75 °C.

$$D_i = D_0\, e^{(-E_a/RT)} \quad (21)$$

From Figure 9 of the intraparticle diffusion model, it was found that the q_t versus $t^{1/2}$ curve passed through the origin which indicates intraparticle diffusion is the rate-controlling step as mentioned earlier. It was observed that R^2 values were closer to 0.99 at all temperatures except at 100 °C and intraparticle rate constant k_{int} increased with increase in temperature up to 75 °C. This can be attributed to enhanced pore diffusion in sorbent particles with an increase in temperature, and it is likely that a large number of CO_2 molecules diffuse into the pore earlier to its being adsorbed. While at 100 °C, the CO_2 molecules would rather get agitated more in the gas film instead of diffusing into the particle pores. Also, the intraparticle diffusion coefficient is calculated according to eq 17 and the values are tabulated in Table 5.

Figure 10 shows the CO_2 desorption of PEI impregnated zeolite 13X at 75 °C and with 60 wt % amine loading along with the curves generated by fitting the two models mentioned earlier. Kinetic parameters and the squared correlation

Table 6. Value of Activation Energy for 13-PEI-60 at 75 °C

model	E_a (kJ/mol)
Avrami's model	35
Boyd model	38

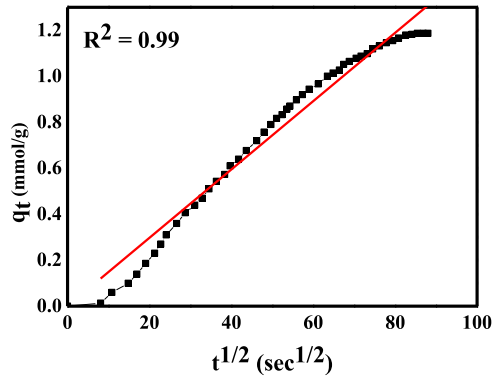

Figure 9. Curve fitting of the intraparticle diffusion model for 13X-PEI-60 at 75 °C.

Table 5. Kinetic Parameters of Diffusion-Based Models by the 13X-PEI-60 Sorbent

model	parameter	25 °C	50 °C	75 °C	100 °C
Boyds model	B [s^{-1}]	0.0001	0.0002	0.0004	0.0027
	D_i [10^{-13}·cm^2/s]	4.05	8.11	16.2	109
	R^2	0.8246	0.8511	0.9369	0.9345
intra-particle	k_{int} [mmol/g·$s^{-1/2}$]	0.01333	0.0156	0.01584	0.001509
	$t_{1/2}$ [$s^{1/2}$]	1576.235	1700	2788.277	354.1332
	D_p [10^{-13}·cm^2/s]	7.61	7.06	4.3	33.9
	R^2	0.9979	0.9854	0.9748	0.5544

DOI: 10.1021/acsomega.9b02047
ACS Omega 2019, 4, 16441−16449

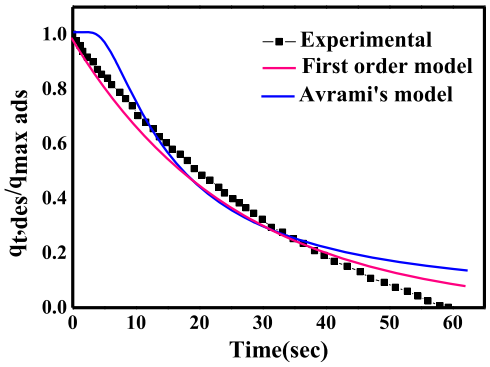

Figure 10. Desorption behavior predicted by different diffusion kinetic models at 75 °C of 13X-PEI-60.

coefficient (R^2) are listed in Table S3. From the R^2 values, it can be concluded that the simple first-order kinetic model displays the best fit which describes the desorption behavior of CO_2 for the studied adsorbent.

In summary, PEI-impregnated 13X zeolite's CO_2 adsorption capacity increases with an increase in temperatures up to 75 °C and thereafter decreases. CO_2 adsorption capacity with PEI loading increases as the loading increases up to 60 wt % and thereafter decreases because of heavy pore blocking in the zeolite 13X framework. The adsorption kinetics was found to fast at 75 °C temperature with 60 wt % PEI loaded sorbent. The mechanism involved is predominantly chemisorption-based, where the primary and secondary amines of PEI reacts with CO_2 to form carbamates as shown in eqs 22 and 23.[38]

$$CO_2 + R_1NH_2 \leftrightarrow R_1NHCOO^- + H^+ \quad (22)$$

$$CO_2 + 2R_1R_2NH \leftrightarrow R_1R_2NCOO^- + R_1R_2NH_2^+ \quad (23)$$

4. CONCLUSIONS

Zeolite 13X has been impregnated with PEI using the methanol solvent. Texture and surface chemistry of the thus-prepared material has been investigated through N_2 adsorption−desorption studies, SEM, XRD, TGA, FTIR, and CHNS analysis. The optimal adsorption temperature of PEI-impregnated zeolite 13X sorbents was found to be 75 °C with the highest CO_2 adsorption and fast kinetics. The optimal PEI loading was found at 60 wt % with a maximum CO_2 adsorption capacity of 1.22 mmol/g in pure atmospheric CO_2. Through kinetic modeling, it can be demonstrated that the CO_2 adsorption onto the PEI impregnated zeolite 13X surface could be accurately described by Avrami's fractional order accurately and intra-diffusion step to be the rate-limiting step for this adsorption process. Thus, it is found that the 60 wt % PEI-modified 13X zeolite showed betterment in CO_2 adsorption capacity over unmodified zeolite 13X by a factor of 2.3 at 75 °C when compared with the available literature on pristine zeolite 13X.[19] The significance of the work lies in the fact that branched PEI impregnated on zeolite could trigger higher adsorption capacity at optimum reaction parameters as reiterated further from the kinetic modelling study. The present study is believed to be a cost-effective approach that can be extended to simulated flue gas conditions for a broad scope of the CO_2 capture study application. Further studies on the impregnation of different molecular weights of PEI amine on zeolite, along with the effect of the binder on palletization in a simulated flue gas conditions would help in demonstrating these adsorbents role better in mitigating climate change by capturing CO_2 in a simple and economical approach.

4.1. Experimental: CO_2 Adsorption and Desorption Studies. CO_2 adsorption/desorption studies were performed by using thermal gravimetric analyzer (TA Instruments SDT Q600) which gives results in the form of CO_2 uptake (in mg) with respect to time under the maintained desired conditions.[25,26] 99.99% pure CO_2 gas was used for CO_2 adsorption measurements. Pure N_2 gas was used as a purge gas in the pretreatment and desorption step. The sample was properly ground to achieve the uniform particle size, and then, 15−20 mg of the sample is loaded on an alumina pan. Before starting the adsorption process, the samples were pretreated at 100 °C in the presence of N_2 gas flow at a flow rate of 50 mL/min, to ensure volatilization of moisture and other volatiles present in the sample. After holding the sample for 60 min, the instrument was allowed to cool down to the desired temperatures which were 25, 50, 75, and 100 °C. As the temperature was equilibrated to desired levels, the gas was switched from pure N_2 to pure CO_2 at a flow rate of 50 mL/min. The CO_2 adsorption process begins and isothermal conditions were maintained for a period of 120 min. Then, the temperature was increased from a set temperature to 105 °C and the gas was switched back to N_2 gas to desorb all the adsorbed CO_2 from the sample. This desorption temperature was maintained for 60 min. The amount of CO_2 molecules adsorbed onto the synthesized modified zeolite (mg/g) was calculated based on eq 24, where w_t and w_0 represents the mass of adsorbent at time t and original mass of the adsorbent, respectively.

$$CO_2 \text{ adsorption} = \frac{w_t(\text{mg}) - w_0(\text{mg})}{w_0(\text{g})} \quad (24)$$

■ ASSOCIATED CONTENT

Supporting Information

The Supporting Information is available free of charge on the ACS Publications website at DOI: 10.1021/acsomega.9b02047.

Adsorption capacity and amine adsorption efficiency measured in pure CO_2 at 75 °C and 1 atm. CO_2 adsorption capacity of different loadings of PEI on zeolite 13X at different temperatures. Desorption kinetic parameters. SEM and TEM Images of 13X zeolite and PEI-modified 13X zeolite. Explanation on FTIR and figure of IR spectra of 13X zeolite and PEI-modified 13X zeolite. Explanation on XRD and figure of the XRD diffractometer for zeolite 13X and PEI-modified zeolite. TGA profile of the adsorbents (PDF)

■ AUTHOR INFORMATION

Corresponding Author

*E-mail: upal03@gmail.com.

ORCID

Swetha Karka: 0000-0003-0680-5283
Sudarshan Kodukula: 0000-0003-2085-9819
Ujjwal Pal: 0000-0002-2110-4242

Notes

The authors declare no competing financial interest.

DOI: 10.1021/acsomega.9b02047
ACS Omega 2019, 4, 16441−16449

■ ACKNOWLEDGMENTS

The authors thank the funding by the Department of Science and Technology (DST), India, (Project code: TMD/CERI/CleanCoal/2017/32) and Indian Institute of Chemical Technology (IICT), Hyderabad, India, for providing their research facilities. Manuscript Communication Number: IICT/Pubs./2019/161.

■ REFERENCES

(1) Huisingh, D.; Zhang, Z.; Moore, J. C.; Qiao, Q.; Li, Q. Recent Advances in Carbon Emissions Reduction: Policies, Technologies, Monitoring, Assessment and Modeling. *J. Clean. Prod.* **2015**, *103*, 1−12.

(2) *Coal—Energy for Sustainable Development*; London, U.K., 2012.

(3) IPCC. *IPCC Special Report on Carbon Dioxide Capture and Storage*, 2005.

(4) Hasan, M. M. F.; First, E. L.; Boukouvala, F.; Floudas, C. A. A Multi-Scale Framework for CO_2 Capture, Utilization, and Sequestration: CCUS and CCU. *Comput. Chem. Eng.* **2015**, *81*, 2−21.

(5) Cuéllar-Franca, R. M.; Azapagic, A. Carbon Capture, Storage and Utilisation Technologies: A Critical Analysis and Comparison of Their Life Cycle Environmental Impacts. *J. CO2 Util.* **2015**, *9*, 82−102.

(6) Ansari, M. B.; Park, S.-E. Carbon Dioxide Utilization as a Soft Oxidant and Promoter in Catalysis. *Energy Environ. Sci.* **2012**, *5*, 9419−9437.

(7) Leung, D. Y. C.; Caramanna, G.; Maroto-Valer, M. M. An Overview of Current Status of Carbon Dioxide Capture and Storage Technologies. *Renew. Sustain. Energy Rev.* **2014**, *39*, 426−443.

(8) Spigarelli, B. P.; Kawatra, S. K. Opportunities and Challenges in Carbon Dioxide Capture. *J. CO2 Util.* **2013**, *1*, 69−87.

(9) Akhtar, F.; Andersson, L.; Keshavarzi, N.; Bergström, L. Colloidal Processing and CO_2 Capture Performance of Sacrificially Templated Zeolite Monoliths. *Appl. Energy* **2012**, *97*, 289−296.

(10) Lv, X.; Li, L.; Tang, S.; Wang, C.; Zhao, X. High CO_2/N_2 and CO_2/CH_4 Selectivity in a Chiral Metal-Organic Framework with Contracted Pores and Multiple Functionalities. *Chem. Commun.* **2014**, *50*, 6886−6889.

(11) Plaza, M. G.; González, A. S.; Pevida, C.; Pis, J. J.; Rubiera, F. Valorisation of Spent Coffee Grounds as CO2 Adsorbents for Postcombustion Capture Applications. *Appl. Energy* **2012**, *99*, 272−279.

(12) Plaza, M. G.; González, A. S.; Pis, J. J.; Rubiera, F.; Pevida, C. Production of Microporous Biochars by Single-Step Oxidation: Effect of Activation Conditions on CO_2 Capture. *Appl. Energy* **2014**, *114*, 551−562.

(13) Broda, M.; Müller, C. R. Sol-Gel-Derived, CaO-Based, ZrO_2-Stabilized CO_2 Sorbents. *Fuel* **2014**, *127*, 94−100.

(14) Valverde, J. M.; Sanchez-Jimenez, P. E.; Perejon, A.; Perez-Maqueda, L. A. Constant Rate Thermal Analysis for Enhancing the Long-Term CO2 Capture of CaO at Ca-Looping Conditions. *Appl. Energy* **2013**, *108*, 108−120.

(15) Xu, X.; Song, C.; Andresen, J. M.; Miller, B. G.; Scaroni, A. W. Novel Polyethylenimine-Modified Mesoporous Molecular Sieve of MCM-41 Type as High-Capacity Adsorbent for CO_2 Capture. *Energy Fuels* **2002**, *16*, 1463−1469.

(16) Jadhav, P. D.; Chatti, R. V.; Biniwale, R. B.; Labhsetwar, N. K.; Devotta, S.; Rayalu, S. S. Monoethanol Amine Modified Zeolite 13X for CO_2 Adsorption at Different Temperatures. *Energy Fuels* **2007**, *21*, 3555−3559.

(17) Su, F.; Lu, C.; Kuo, S.-C.; Zeng, W. Adsorption of CO_2 on Amine-Functionalized y-Type Zeolite. *Energy Fuels* **2010**, *24*, 1441−1448.

(18) Xu, X.; Zhao, X.; Sun, L.; Liu, X. Adsorption Separation of Carbon Dioxide, Methane and Nitrogen on Monoethanol Amine Modified β-Zeolite. *J. Nat. Gas Chem.* **2009**, *18*, 167−172.

(19) Chatti, R.; Bansiwal, A. K.; Thote, J. A.; Kumar, V.; Jadhav, P.; Lokhande, S. K.; Biniwale, R. B.; Labhsetwar, N. K.; Rayalu, S. S. Amine Loaded Zeolite for Carbon Dioxide Capture: Amine Loading and Adsorption Studies. *Microporous Mesoporous Mater.* **2009**, *121*, 84−89.

(20) Bezerra, D. P.; Silva, F. W. M. D.; Moura, P. A. S. D.; Sousa, A. G. S.; Vieira, R. S.; Rodriguez-Castellon, E.; Azevedo, D. C. S. CO_2 Adsorption in Amine-Grafted Zeolite 13X. *Appl. Surf. Sci.* **2014**, *314*, 314−321.

(21) Chen, C.; Kim, S.-S.; Cho, W.-S.; Ahn, W.-S. Polyethylenimine-Incorporated Zeolite 13X with Mesoporosity for Post-Combustion CO_2 Capture. *Appl. Surf. Sci.* **2015**, *332*, 167−171.

(22) Shen, X.; Du, H.; Mullins, R. H.; Kommalapati, R. R. *Polyethylenimine Applications in Carbon Dioxide Capture and Separation : From Theoretical Study to Experimental Work*; John Wiley & Sons, Inc., 2017; pp 822−833.

(23) Li, K.; Jiang, J.; Yan, F.; Tian, S.; Chen, X. The Influence of Polyethyleneimine Type and Molecular Weight on the CO 2 Capture Performance of PEI-Nano Silica Adsorbents. *Appl. Energy* **2014**, *136*, 750−755.

(24) Xu, X.; Song, C.; Andrésen, J. M.; Miller, B. G.; Scaroni, A. W. Preparation and Characterization of Novel CO_2 "Molecular Basket" Adsorbents Based on Polymer-Modified Mesoporous Molecular Sieve MCM-41. *Microporous Mesoporous Mater.* **2003**, *62*, 29−45.

(25) Rashidi, A. N.; Yusup, S.; Hon, L. Kinetic Studies on Carbon Dioxide Capture Using Activated Carbon. *Chem. Eng. Trans.* **2013**, *35*, 361−366.

(26) Liu, Z.; Pudasainee, D.; Liu, Q.; Gupta, R. Post-Combustion CO_2 Capture Using Polyethylenimine Impregnated Mesoporous Cellular Foams. *Sep. Purif. Technol.* **2015**, *156*, 259−268.

(27) Qiu, H.; Lv, L.; Pan, B.-c.; Zhang, Q.-j.; Zhang, W.-m.; Zhang, Q.-x. Critical Review in Adsorption Kinetic Models. *J. Zhejiang Univ., Sci., A* **2009**, *10*, 716−724.

(28) Zhang, Z.; Huang, S.; Xian, S.; Xi, H.; Li, Z. Adsorption Equilibrium and Kinetics of CO_2 on Chromium Terephthalate MIL-101. *Energy Fuels* **2011**, *25*, 835−842.

(29) Liu, Q.; Shi, J.; Zheng, S.; Tao, M.; He, Y.; Shi, Y. Kinetics Studies of CO_2 Adsorption/Desorption on Amine-Functionalized Multiwalled Carbon Nanotubes. *Ind. Eng. Chem. Res.* **2014**, *53*, 11677−11683.

(30) Ohs, B.; Krödel, M.; Wessling, M. Adsorption of Carbon Dioxide on Solid Amine-Functionalized Sorbents: A Dual Kinetic Model. *Sep. Purif. Technol.* **2018**, *204*, 13−20.

(31) Kajjumba, G. W.; Emik, S.; Öngen, A.; Kurtulus Özcan, H.; Aydın, S. Modelling of Adsorption Kinetic Processes—Errors, Theory and Application. *Adv. Sorption Process Appl.* **2018**, DOI: 10.5772/intechopen.80495.

(32) Yakout, S. M.; Elsherif, E. Batch Kinetics, Isotherm and Thermodynamic Studies of Adsorption of Strontium from Aqueous Solutions onto Low Cost Rice-Straw Based Carbons. *Carbon: Sci. Technol.* **2010**, *3*, 144−153.

(33) Al-Marri, M. J.; Kuti, Y. O.; Khraisheh, M.; Kumar, A.; Khader, M. M. Kinetics of CO_2 Adsorption/Desorption of Polyethylenimine-Mesoporous Silica. *Chem. Eng. Technol.* **2017**, *40*, 1802−1809.

(34) Zhang, Z.; Xiao, Y.; Wang, B.; Sun, Q.; Liu, H. Waste Is a Misplayed Resource: Synthesis of Zeolite from Fly Ash for CO2 Capture. *Energy Procedia* **2017**, *114*, 2537−2544.

(35) Hicks, J. C.; Drese, J. H.; Fauth, D. J.; Gray, M. L.; Qi, G.; Jones, C. W. Designing Adsorbents for CO_2 Capture from Flue Gas-Hyperbranched Aminosilicas Capable of Capturing CO_2 Reversibly. *J. Am. Chem. Soc.* **2008**, *130*, 2902−2903.

(36) Wei, M.; Yu, Q.; Duan, W.; Hou, L.; Liu, K.; Qin, Q.; Liu, S.; Dai, J. Equilibrium and Kinetics Analysis of CO_2 Adsorption on Waste Ion-Exchange Resin-Based Activated Carbon. *J. Taiwan Inst. Chem. Eng.* **2017**, *77*, 161−167.

(37) Karthikeyan, S.; Sivakumar, B.; Sivakumar, N. Film and Pore Diffusion Modeling for Adsorption of Reactive Red 2 from Aqueous Solution on to Activated Carbon Preparedfrom Bio-Diesel Industrial Waste. *E-J. Chem.* **2010**, *7*, S175−S184.

(38) Lee, S.-Y.; Park, S.-J. A Review on Solid Adsorbents for Carbon Dioxide Capture. *J. Ind. Eng. Chem.* **2015**, *23*, 1−11.

DOI: 10.1021/acsomega.9b02047
ACS Omega 2019, 4, 16441−16449